Asociación Argentina de Mecánica Computacional

Mecánica Computacional Vol XXIX, págs. 8807-8817 (artículo completo)
Eduardo Dvorkin, Marcela Goldschmit, Mario Storti (Eds.)
Buenos Aires, Argentina, 15-18 Noviembre 2010

ANALISYS OF OIL WELL DRILLING DYNAMICS FROM NON-SMOOTH MODELS

Mariana N. Vasconcellos and Marcelo A. Savi

Federal University of Rio de Janeiro, COPPE - Department of Mechanical Engineering,P.O. Box 68.503, 21.941.972 - Rio de Janeiro - RJ, Brazil, mariananv@gmail.com, savi@mecanica.ufrj.br

Keywords: Nonlinear dynamics, stick-slip, bit bounce, drill-string.

Abstract. Drill-string vibration is one of the most undesirable problems that occur during the oil-well drilling operation. The control of this vibration is essential because they may cause low performace of the drilling, damage and failure of the drill-string and well problems. In this work, we present a coupled non-smooth two-degree of freedom system to model drilling vibrations, developing a parametric analysis of the drill-string vibrations. Special attention is dedicated to the bit/formation interaction, which is considered as the main external force. Moreover, we investigate the transitions between different phases of motion and the non-smooth dynamics associated with the stick-slip and bit-bounce. We adopt smooth functions that presents advantages in terms of mathematical description and numerical analysis. The undertaken numerical simulations show that the developed mathematical model is capable of predicting a full range of dynamic responses including the non-smooth behavior including stick-slip and bit-bounce responses. Experimental data is used as a reference for numerical simulations.

1 INTRODUCTION

The oil-well drilling is a complex and very expensive operation being related to the knowledge of several aspects of engineering and geoscience. The drilling process has a significant influence on the cost of the exploration process. Thus, the budget for the development of a field and its operations must be carefully planned so that the well can be drilled safely and profitably.

A drill-string can be modeled as a non-smooth system by considering contact and non-contact with the rock during operation. Basically, drill-string vibration analysis can be split in three modes: axial, torsional and flexural. Concerning non-smooth phenomena, the axial mode is related to the constant impact of the drill with the background well. The torsional mode is associated with the dry friction between the bit and the well. Finally, the lateral mode is related to the impact of the Bottom Hole Assembly (BHA) with the borehole wall. Although these models are essentially coupled, they are usually treated separatelly. Neverthelless, the coupling among these modes is essential to describe some important phenomena during drilling (Christoforou and Yigit, 2003; Leine, 2000; Spanos et al., 1995).

Divenyi (2009) developed an analysis of drill-string vibration that was capable of predicting a full range of dynamic responses including the non-smooth behaviour. Two fundamental phenomena were of concern: bit-bounce and stick-slip.The mathematical model is based on the Christoforou and Yigit (2003) that considers a coupling between axial and torsional vibrations. Here, the nonlinear dynamics of this system is revisited in order to investigate the influence of different system parameters especially the ones related to the formation in the drill-string vibration. Experimental data is used as a reference for numerical simulations.

2 MATHEMATICAL MODEL

The model here presented was originally proposed by Christoforou and Yigit (2003) and investigated by Divenyi (2009) in order to describe the dynamical behavior of a drill-string. The model assumes a two degrees-of-freedom model that couples the axial and the torsional vibrations. The drill-string is treated as a lumped parameter system, so that the equations are simplified to ordinary differential equations. The forcing comes from the bit and formation interaction, being related to the strings rotational movement. The torsional forcing is given by the friction between the bit and the rock and the cutting torque acting on the bit. The coupling between axial and torsional modes is given by the bit/rock interaction, which generates the forcing in the axial direction.

The proposed model treats the BHA as a lumped mass at the bottom of the drill-string. The axial mass, m_a , is given by the sum of the BHA and the equivalent mass of the drill-pipes. The drill-string stiffness is given by the drill-pipes, in such way that BHA is considered as a rigid body. This hypothesis is based on the fact that the transversal section of the BHA is greater than the drill-pipes, and the length of the drill-pipes is greater than the BHA. Under this assumption, it is assumed that k_a is the stiffness of the axial movement and c_a is the linear viscous damping coefficient.

The axial displacement is denoted by the x variable. The origin of the axial movement is considered at the moment that $x = 0$, in other words, when the bit is tangent to the rock and the bit exerts zero force on the formation. In this point, the traction force applied in the BHA is equal to the weight. In the axial degree-of-freedom, we also considered the static equilibrium, with the nominal Weight-On-Bit (WOB) $\underline{F}_b$ applied, but without drill-string rotation. $\underline{F}_b$ is called nominal WOB because during the dynamic response of the system this WOB varies. The static displacement in the x direction, is related with the drill-bit penetration in the rock when

WOB equals $\underline{F}_b$. Since the weight is applied on the drill-bit, the traction also varies during the dynamical response.

The torsional degree-of-freedom is analysed by considering that torsional stiffness is provided by the drill pipes,k_t, in such way that the BHA does not receive any torsion. The torsional inertia is composed by a combination of BHA and drill-pipes, I_t. Besides, the torsional model assumes a linear viscous damping, c_t and the rotation angle is represented by ϕ.

Under these assumptions, the system dynamics is represented by the following equations:

$$\begin{cases} m_a\ddot{x} + c_a\dot{x} + k_a x = F_0 - WOB \\ I_t\ddot{\phi} + c_t\dot{\phi} + k_t(\phi - \phi_{mr}) = -TOB \end{cases} \tag{1}$$

The Weight-On-Bit (WOB) and Torque-On-Bit(TOB) can be defined according the contact and non-contact with the formation.

$$WOB = \begin{cases} k_c(x - s_0\sin(n_b\phi)), & \text{with contact} \\ 0, & \text{without contact} \end{cases} \tag{2}$$

$$TOB = \begin{cases} WOB(\frac{2}{3}f(\dot{\phi}) + \zeta\sqrt{r_c\delta_c}), & \text{with contact} \\ 0, & \text{without contact} \end{cases} \tag{3}$$

The coupling between axial and torsional oscillations is through the contact with the formation where the axial force is the catalyst to generate a resistive torque. Specifically, during the contact when drill-bit rotates, n_b represents the general characteristic of the drilling. Basically, its definition is related to the number of elevations (peaks) of the formation for a complete bit rotation. Therefore, a tri-cone bit has $n_b = 3$ while a PDC bit has $n_b = 1$.

The torque acting on the drill-bit is modelled by two terms: the first one is related to the dry friction existing between the bit and the formation; and the second one is related to the torque needed to cut the rock. The equation proposed by Spanos et al. (1995) is employed to desccribe this behaviour. Note that the friction is considered to be evenly distributed on the front face of the bit; r_h is the drill-bit radius, δ_c is the average cutting depth,ζ is a dimensionless parameter that characterizes the force necessary to cut the rock.

The definition of the stiffness for an oil well drilling with PDC bit can be defined by the model proposed by Hareland and Rampersad (1994):

$$k_c = \frac{\underline{F}_b}{N_s A_p} \tag{4}$$

where A_p and A_v are respectively the projected area and the area in front of the cutter and N_s is the numbers of cutter.

$$A_p = \sin\theta\left[\left(\frac{d_c}{2}\right)^2\cos^{-1}\left(1 - \frac{2\delta_c}{\cos\theta d_c}\right) - \sqrt[2]{\left(\frac{d_c\delta c}{\cos\theta} - \frac{\delta_c^2}{\cos^2\theta}\right)}\left(\frac{d_c\delta_c}{2\cos\theta}\right)\right] \tag{5}$$

$$A_v = \cos\alpha\sin\theta\left[\left(\frac{d_c}{2}\right)^2\cos^{-1}\left(1 - \frac{2\delta_c}{\cos\theta d_c}\right) - \sqrt[2]{\left(\frac{d_c\delta c}{\cos\theta} - \frac{\delta_c^2}{\cos^2\theta}\right)}\left(\frac{d_c\delta_c}{2\cos\theta}\right)\right] \tag{6}$$

where θ and α are respectively the PDC cutter backrake and siderake angle (deg).

$$ROP = \frac{A_v 14.14 N_s \omega_{mr}}{d_h} \tag{7}$$

Moreover, the following equation are employed for the estimation of the rate of penetration and depth of cutting (Christoforou and Yigit, 2003).

$$ROP = c_1 \underline{F}_b \sqrt{\omega_{mr}} + c_2 \tag{8}$$

$$\delta_c = \frac{2\pi ROP}{\omega_{mr}} \tag{9}$$

where $\underline{F}_b = k_c \underline{x}$, with $\underline{x}$ representing the bit teeth penetration into the formation when $WOB = \underline{F}_b$; c_1 and c_2 are constants.

This system has two sources of non-smootheness. Dry friction between the formation and the drill-bit is one of these that can be treated by a continuous function of the angular velocity (Leine, 2000):

$$f(\dot{\phi}) = -sign(\dot{\phi})\frac{2}{\pi}arcatan(\varepsilon\dot{\phi})\left(\frac{\mu_e - \mu_d}{1 + \tau\|\dot{\phi}\|}\right) \tag{10}$$

In this equation, the constants μ_e and μ_d are the static and dynamic friction coefficients, respectively; ε and τ are dimensionless numerical constants, where $\varepsilon \gg 1$ and $\tau > 0$. These constants are responsible for the proper transition from $-\mu_d$ to $+\mu_d$. If properly chosen, these constants can get the smoothened shape of the dry friction really close to that of its original non-smooth function.

The other non-smootheness is due to the contact/non-contact behavior. In this case, the same procedure used in Savi et al. (2007) can be employed in order to smoothness the governing equations. This idea defines a transition region with thickness, η, and under these assumptions, the system is governed by the following equations.

For the contact region, where $x \geq s_0 \sin(n_b\phi) + \eta$:

$$\begin{cases} m_a\ddot{x} + c_a\dot{x} + k_a x = F_0 - k_c(x - s_0\sin(n_b\phi)) \\ I_t\ddot{\phi} + c_t\dot{\phi} + k_t(\phi - \phi_{mr}) = -k_c(x - s_0\sin(n_b\phi))(\frac{2}{3}f(\dot{\phi}) + \zeta\sqrt{r_c\delta_c}) \end{cases} \tag{11}$$

For the non-contact region, where $x \leq s_0 \sin(n_b\phi) - \eta$:

$$\begin{cases} m_a\ddot{x} + c_a\dot{x} + k_a x = F_0 \\ I_t\ddot{\phi} + c_t\dot{\phi} + k_t(\phi - \phi_{mr}) = 0 \end{cases} \tag{12}$$

For the transition region, where $s_0 \sin(n_b\phi) - \eta < x < s_0 \sin(n_b\phi) + \eta$:

$$\begin{cases} m_a\ddot{x} + c_a\dot{x} + k_a x = F_0 - k_c(x - s_0 sen(n_b\phi) + \eta) \\ I_t\ddot{\phi} + c_t\dot{\phi} + k_t(\phi - \phi_{mr}) = -k_c(\frac{2}{3}f(\dot{\phi})r_h\eta + \zeta\sqrt{r_c\delta_c}(\frac{x - s_0 sen(n_b\phi) + \eta}{2}) \end{cases} \tag{13}$$

3 NUMERICAL SIMULATIONS

Numerical results obtained using the proposed model are discussed in this section. Table 1 presents parameters employed for all simulations. Experimental results from a reservoir section are used as a reference. The well is related to a 12 $1/4$" reservoir section that has a 8" diameter. Four different lythologies are of concern acording to the depth: shale, basalt , sandstone and limestone. Each one has specific properties. The drilling process uses a PDC bit and Figure 1 presents real data employed to perform numerical simulation and also results obtained from the proposed model. The graphs in the green box represent $\underline{F}_b$ and ω_{mr} experimental values of the well data. The blue box represents k_c values calculated by the Hareland and Rampersad

(1994) equation for oil well drilling with PDC bits. The black box presents results obtained by the numerical integration of the mathematical model for ROP and bifurcation diagrams.

The bifurcation diagram represents the maximum values of the axial displacement x (x_{max}) under the slow quasi-static variation of the oil well depth (l). Moreover, this diagram indicates the ocurrence of the bit-bounce behaviour, represented by blue points, and stick-slip behaviour, represented by green circles. The left side labels represent the response from the numerical simulation while the right side is related to experimental data. The evaluation of these phenomena considers the following criteria: bit-bounce behaviour occurs when $x \leq s_0 \sin(n_b\phi)$; and stick-slip behaviour occurs when $\dot{\phi} \leq 0.0004$.

The next sections show some behaviours for specific oil well depth (l). Basically, we present results related to normal condition operation, bit-bounce and stick-slip.

Table 1: Drilling parameters.

c_1	c_2	η	τ	ε	N_s	α	β
1.35×10^{-8}	-1.9×10^{-4}	10^{-6}	10.9	10^4	65	10	10

l_{BHA}	d_i	d_e	dc_i	dc_e	d_p
(m)	(pol)	(pol)	(pol)	(pol)	(pol)
200	8	3	8	3	12.25
-	(mm)	(mm)	(mm)	(mm)	(mm)
-	203.2	76.2	203.2	76.2	311.15

ρ_{fl}	μ_{fld}	c_{ma}	c_a	s_0	n_b	μ_e	μ_d	ζ
(lb/gal)	(cP)	-	-	(mm)	-	-	-	-
12.5	200	1.7	4000	0.01	-	-	-	-
(kg/m_3)	$Pa.s$	-	-	-	-	-	-	-
1497.83	0.2	-	-	-	-	-	-	-

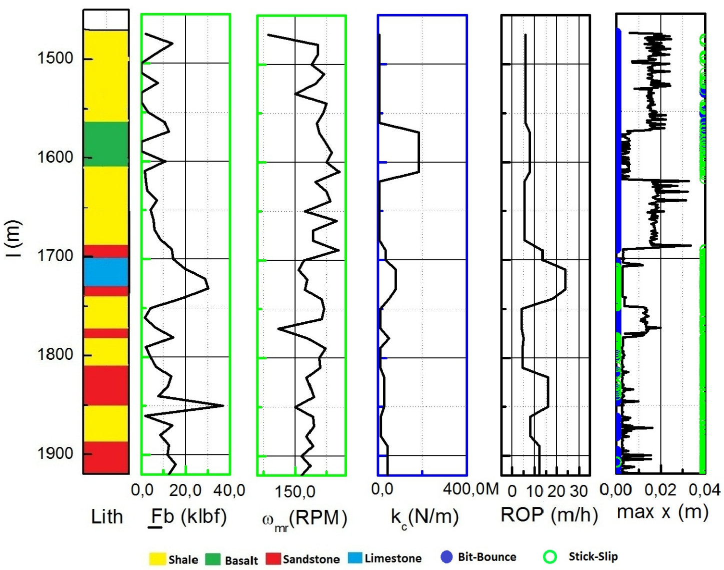

Figure 1: Simulation reservoir section.

3.1 Normal Condition

In order to observe the general behaviour of the shale lithology, we present an amplification of the previous bifurcation diagram (Figure 2). Once again, the left side label indicates the bit-bounce and stick-slip behaviours obtained with the numerical simulation (blue and green circles, respectively) while the right side labels show the experimental data for these behaviours.

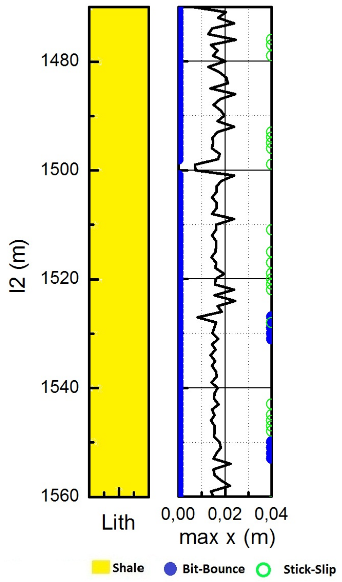

Figure 2: Bifurcation diagram of shale lithology from the depth of 1470 m until 1560 m

Initially, dynamic response for normal conditions are computed for a depth of 1500 m in shale lithology. In this simulation we consider a $\omega_{mr} = 163.1RPM$, $\underline{F}_b = 4.395klbf$ and $k_c = 6 \times 10^6 N/m$. Under these conditions, the bifurcation diagram indicates a normal behaviour, without stick-slip and bit-bounce, the same behaviour of experimental data. Figure 3 presents steady state response for this situation showing a regular drilling operation, without severe vibrations. Figure 3a and 3b show phase spaces for axial and torsional motion. Discontinuities are not present in both phase spaces, which indicates that there is no bit-bounce, and therefore the bit does not loose contact with the formation. The torsional phase space does not present situations where $d\phi/dt$ vanishes, and therefore there is no stick-slip. One can deduce that this behaviour is periodic and bounded, which means that the drilling takes place without severe vibration. Figure 3c shows the angular displacement ϕ and ϕ_{mr} as a function of time. We can observe that both curves are almost the same and that along the drill-string moviment with continuously rotating, ϕ always increases, fluctuating around ϕ_{mr} value. Another way of visualizing the behaviour of ϕ is through the difference between $\phi_{mr} - \phi$ against time, represented in Figure 3d. We can obtain the angular distance between the bit and the rotary table, which indicates how much the rotary table is ahead of the drill-bit.

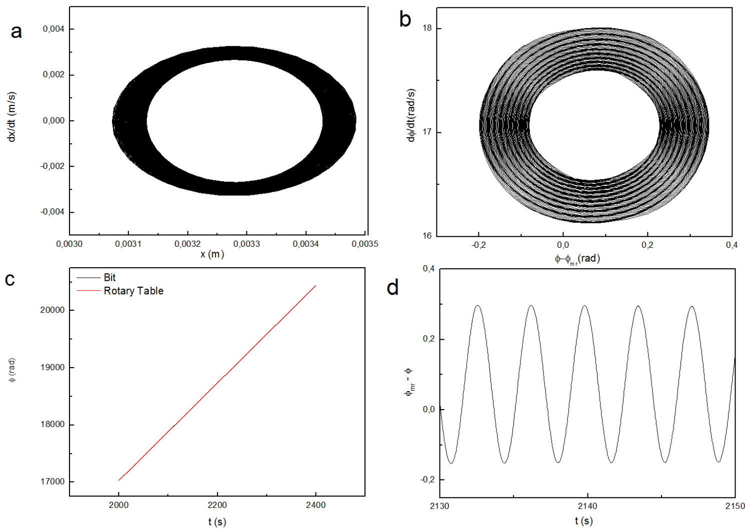

Figure 3: (a) Phase portrait for axial and (b) torsional vibration for the normal condition.(c) Drill-bit and rotary table angular displacement in time.(d) Difference between angular displacement of the drill-bit and rotary table.

3.2 Stick-Slip

The general behaviour of the shale lithology is evaluated by considering an amplification of the bifurcation diagram (Figure 4). The left side label indicates the bit-bounce and stick-slip behaviours obtained with the numerical simulation (blue and green circles, respectively) while the right side labels show the experimental data for these behaviours.

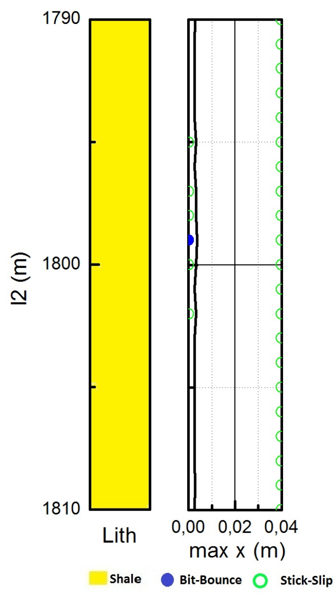

Figure 4: Bifurcation diagram of shale lithology from the depth of 1790 m until 1810 m

Stick-slip behaviour is now of concern. Figure 5 presents stick-slip response by considering $\omega_{mr} = 171RPM$, $\underline{F}_b = 4.29klbf$ and $k_c = 1.09 \times 10^7 N/m$ and a depth of 1800 m in shale lithology. Under these conditions, the bifurcation diagram indicates the occurence of stick-slip phenomenon, the same behaviour of experimental data. Figure 5a and 5b presents phase space for both axial and torsional movement. In the torsional phase portrait we can observe a horizontal line in d$\phi/dt = 0$, representing the situation where the drill-bit stops (stick stage) which indicates the existence of stick-slip. This analysis shows that the phase space is an adequate tool to identify the stick-slip. The axial phase space does not present any discontinuity indicating that the bit-bounce phenomenon does not occur. Figure 5c and 5d shows the time history of angular velocity $d\phi/dt$ and relative angular displacement $\phi_{mr} - \phi$. Figure 5c shows the time intervals in which the angular velocity vanishes, corresponding to the stick stage in which the drill-bit stops rotating. When the stick intervals happens the drill-bit angular velocity is equal zero, however the rotary table continues rotating. Under this condition, we have a greater displacement between the drill-bit and the rotary table (Figure 5d) comparing with the normal condition (Figure 3c). Hence, the large fluctuations of $\phi_{mr} - \phi$ may be related to the stick-slip. Therefore, this behaviour is more adequate to be analysed by the angular velocity or the torsional phase space.

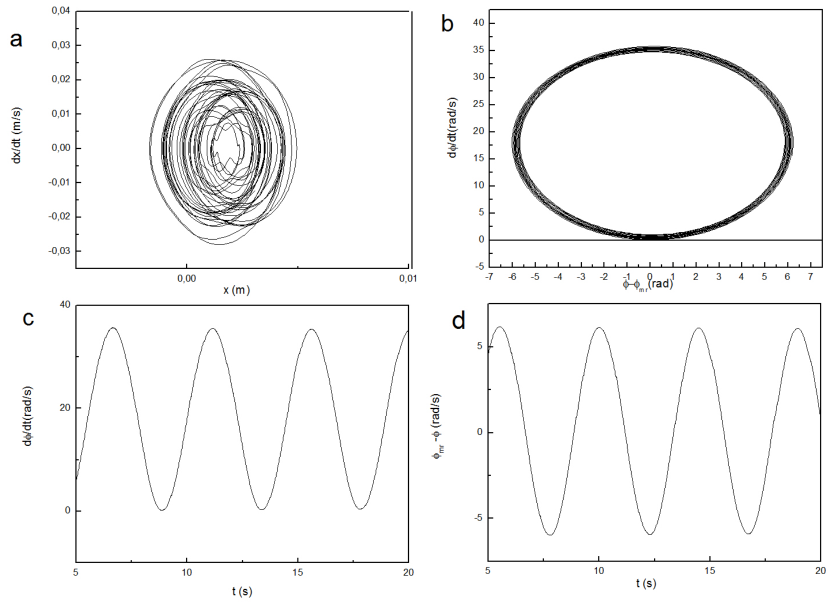

Figure 5: (a) Phase portrait for axial and (b) torsional vibration for stick-slip case.(c)Time histories of angular displacement and (d) relative angular displacement

3.3 Bit-Bounce

Bit-bounce behaviour is now in focus by assuming a depth of 1600 m in basalt lithology. The general behaviour is evaluated by considering an amplification of the bifurcation diagram of the basalt lithology (Figure 6). Where the left side label indicates the bit-bounce and stick-slip behaviours obtained with the numerical simulation (blue and green circles, respectively) while the right side labels show the experimental data for these behaviours.

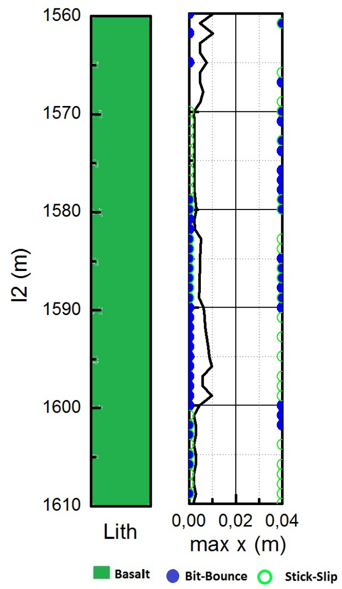

Figure 6: Bifurcation diagram of shale lithology from the depth of 1560 m until 1610 m

By assuming $\omega_{mr} = 176.4RPM$, $\underline{F}_b = 4.96klbf$ and $k_c = 1.83N/m$, the bifurcation diagram indicates the occurence of bit-bounce phenomenon, the same behaviour of experimental data. Figure 7a shows the axial phase space where we can observe two distinct regions, highlighting the non-smoothness related to the bit-bounce. These regions represent the moment that the bit lose and recovery contact. The torsional phase space, on the other hand, shows that there is no stick-slip althought the axial mode discontinuity cannot be observed on the torsional phase space (Figure 7b). Figure 7c and 7d shows the axial displacement and the axial velocity time histories. Comparing to the normal condition case (Figure 3c and 3d) can be observed that the responses are less smooth, having sharper peaks. However, it is not easy to diagnose the bit-bounce existence through these graphs.

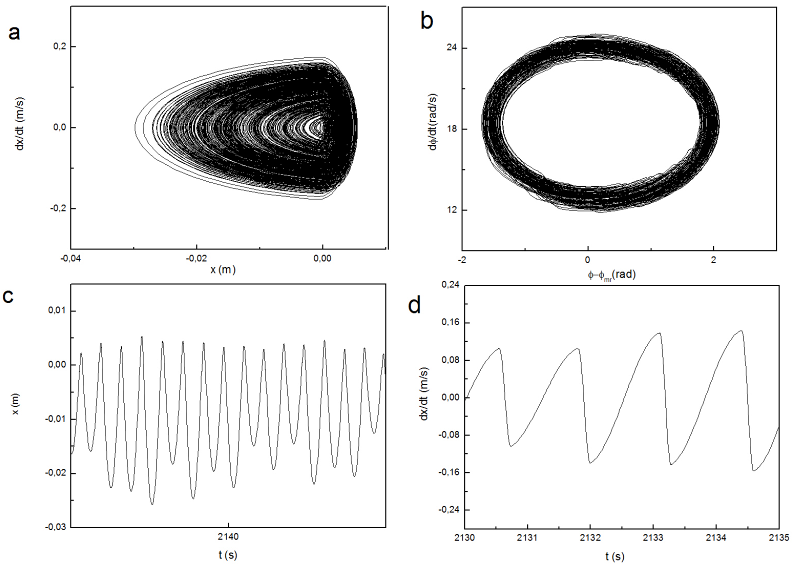

Figure 7: (a) Phase portrait for axial and (b) torsional vibration for the bit-bounce case. (c) Time histories of axial displacement and (d) velocity.

3.4 Bit-bounce and stick-slip behaviours

This section treats a situation where bit-bounce and stick-slip behaviours occur simultaneously. In this simulation we consider a $\omega_{mr} = 176.4RPM$, $\underline{F}_b = 4.96klbf$ and $k_c = 1.83 \times 10^8 N/m$ in a depth of 1580 m in basalt lithology. The bifurcation diagram of this region is shown in Figure (6) that represents an amplification of the original diagram of Figure (1).

Under these conditions, the bifurcation diagram indicates the occurence of stick-slip and bit-bounce phenomena, the same behaviour of experimental data. The axial phase space (Figure 8a) shows the occurence of bit-bounce phenomenon represented by the existence of two distinct regions, indicating the non-smooth characteristic of this phenomenon. Figure 8b shows the torsional phase space, where one can find points with d$\phi/dt = 0$. The analysis of these phase spaces allows one to indentify both behaviours.

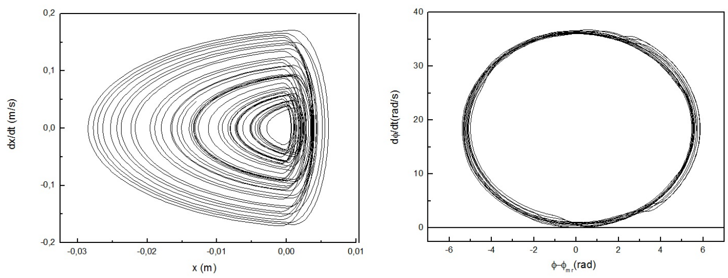

Figure 8: (a) Phase portrait for axial and (b) torsional vibration for the bit-bounce and stick-slip case.

4 CONCLUSIONS

In this paper, we model and analyse the drill-string vibration by a coupled non-smooth two-degree of freedom system. Drill-string vibration is one of the most undesirable problems that occur during the oil-well drilling operation and the control of this vibration is essential because they may cause low performace of the drilling, damage and failure of the drill-string and well problems. The coupling between the axial and torsional modes is given by the bit/rock interaction, which generates the forcing in the axial direction.The forces and torques are defined according the contact or non-contact scenarios, establishing a non-smooth system. Besides, the dry friction between the formation and the drill-bit introduce another non-smoothness to the system. The resulting non-smooth system is treated by promoting the smoothness of the governing equations. We adopt smooth functions which are advantageous in terms of mathematical description and numerical analysis. Especial attention is dedicated to the bit/formation interaction, which is considered as the main external force. Numerical simulations are carried out in different kinds of formation. Our studies have showed that the developed mathematical model is capable of predicting a full range of dynamic responses including the non-smooth behaviour and that the phase spaces and bifurcation digrams are useful to diagnose the bit-bounce and stick-slip behaviours.

5 ACKNOWLEDGEMENTS

The authors would like to acknowledge the support of the Brazilian Research Agencies CNPq and FAPERJ and through the INCT-EIE (National Institute of Science and Technology - Smart Structures in Engineering) the CNPq and FAPEMIG. The Air Force Office of Scientific Research (AFOSR) is also acknowledged.

REFERENCES

Christoforou A.P. and Yigit A.S. Fully coupled vibrations of actively controlled drillstrings. *Journal of Sound and Vibration*, 267(5):1029 – 1045, 2003.

Divenyi S. *Dinâmica de sistemas não-suaves aplicada à perfuração de poços de petróleo*. Master's Thesis, Universidade Federal do Rio de Janeiro, 2009.

Hareland G. and Rampersad P. Drag - bit model including wear. In *SPE Latin America/Caribbean Petroleum Engineering Conference*. Copyright 1994, Society of Petroleum Engineers Inc., Buenos Aires, Argentina, 1994.

Leine R.I. *Bifurcations in Discontinuous Mechanical Systems of Filippov-Type*. Master's Thesis, Technische Universiteit Eindhoven, 2000.

Savi M.A., Divenyi S., Franca L.F.P., and Weber H.I. Numerical and experimental investigations of the nonlinear dynamics and chaos in non-smooth systems. *Journal of Sound and Vibration*, 301(1-2):59 – 73, 2007.

Spanos P.D., Sengupta A.K., Cunningham R.A., and Paslay P.R. Modeling of roller cone bit lift-off dynamics in rotary drilling. *Journal of Energy Resources Technology*, 117(3):197–207, 1995.